Selective Growth of Vertical ZnO Nanowire Arrays Using Chemically Anchored Gold Nanoparticles

Daisuke Ito,[†,*] Michael L. Jespersen,[‡] and James E. Hutchison*

Department of Chemistry and Materials Science Institute, University of Oregon, Eugene, Oregon 97403. [†]Current address: Materials Laboratories, Sony Corporation. [‡]Current address: Nanostructured and Biological Materials Branch, Air Force Research Laboratories (AFRL/RXBN), Wright-Patterson AFB, Ohio.

ABSTRACT A selective growth method for ZnO vertical nanowire arrays is demonstrated using self-assembled gold nanoparticles as the growth catalyst. Gold nanoparticles functionalized with bifunctional (thiol-phosphonic acid) ligands assemble rapidly and selectively onto a patterned ZnO seed layer. Vertical ZnO nanowire arrays are grown by the vapor−liquid−solid (VLS) deposition method from the ZnO seed layer through the catalytic effect of the bound gold nanoparticles. This synthesis method offers a number of advantages for producing ZnO nanowires because it permits selective placement through directed self-assembly of gold nanoparticles, enables rapid growth, eliminates vacuum deposition processing, and minimizes the amount of gold waste when compared to traditional methods that require vapor deposition of gold films.

KEYWORDS: nanowire · nanoparticle · nanofabrication · zinc oxide · gold · green chemistry · self-assembly

Self-assembled nanostructures have attracted much attention due to their wide range of potential applications in optics, electronics, and catalysis.[1−4] Zinc oxide is a particularly attractive material for optical devices that operate at room temperature because ZnO has a wide band gap (3.37 eV) and large exciton binding energy (60 meV). There have been many reports on different types of self-assembled ZnO nanostructures.[5−11] Among these structures, vertically aligned ZnO nanowire arrays are promising candidates for applications in nanoscale transistors,[12] sensors,[13] light emitting devices,[9,14] and field emission devices.[15] In order to realize these and other applications, low-cost techniques are necessary that enable selective growth, permit vertical alignment, and have potential for large-scale fabrication. Recently, aligned ZnO nanowires have been synthesized by various processes, including metal-organic vapor-phase epitaxy,[16] thermal evaporation,[17] electrochemical deposition,[18] and vapor−liquid−solid (VLS) deposition.[19] In each of these deposition processes, a patterned evaporated gold film is used as the catalyst material for selective growth.[19] Although patterned ZnO nanowire arrays show promise for use in novel devices, the use of evaporated gold films as a catalyst presents a couple of disadvantages, including a lack of control over the diameter and density of nanowires within the array and the generation of large amounts of gold waste. The use of self-assembled gold nanoparticle films as catalysts can potentially address these disadvantages,[20] by reducing the amount of gold needed to produce the catalyst film, enabling the site-selective growth of nanowire arrays, and providing opportunities to control structural properties of the nanowire arrays through variation of the areal density and/or size of the nanoparticle precursors. Thus far, growth of ZnO nanowire arrays using self-assembled monolayers of gold nanoparticles has not been described.

In this article, we demonstrate the selective growth of ZnO nanowire arrays using self-assembled films of gold nanoparticles. The particles are modified with a terminally functionalized thiol ligand shell, 2-mercaptoethylphosphonic acid (2-MEPA), which selectively adsorbs onto a patterned ZnO seed layer on SiO_2 or c-sapphire substrates (Figure 1). Because the Zn atoms of the ZnO(0001) surface possess positive charge[21] and the SiO_2 surface is slightly negatively charged in aqueous solutions, the anionic phosphonic acid functionalized gold nanoparticles assemble onto the ZnO surface selectively. Utilizing the seed layer as a pattern and the functionalized gold nanoparticles as catalyst allows one to realize selectively positioned, vertical ZnO nanowire arrays without the disadvantages described for arrays derived from patterned evaporated gold layers.

*Address correspondence to daisukeb.ito@jp.sony.com, hutch@uoregon.edu.

Received for review October 23, 2007 and accepted September 08, 2008.

Published online October 2, 2008.
10.1021/nn800438m CCC: $40.75

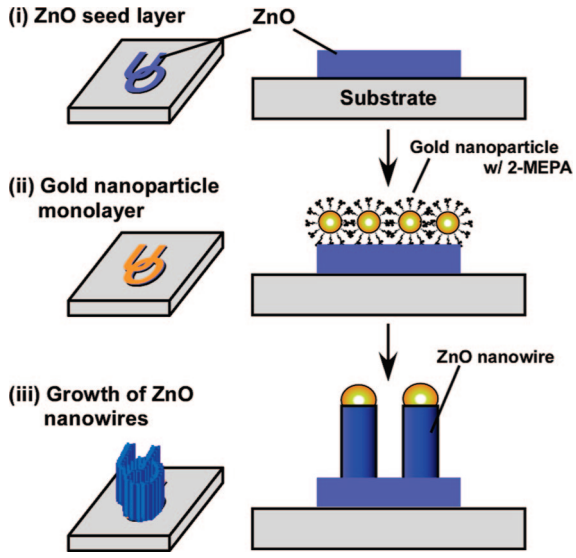

Figure 1. Schematic diagram of selective growth of ZnO nanowires using a chemically anchored array of gold nanoparticle catalysts.

RESULTS AND DISCUSSION

In order to realize site-selective growth of nanowire arrays, it was first necessary to prepare nanoparticle catalysts that would preferentially self-assemble onto a patterned ZnO seed layer and not onto the surrounding SiO_2 substrate. To this end, we synthesized 1.5 nm triphenylphosphine-stabilized gold nanoparticles, which readily undergo ligand exchange reactions with a broad range of ω-functionalized thiols. Figure 2 shows TEM images of gold nanoparticles (a) with a PPh_3 ligand shell and (b) with a 2-MEPA ligand shell following ligand exchange. TEM images indicate that the average diameter and size distribution of gold nanoparticles are similar before and after ligand exchange, exhibiting average diameters of 1.3 and 1.4 nm, respectively. As previously mentioned, the 2-MEPA ligand serves as a linker between the gold nanoparticles and the ZnO surface (Figure 1). Thiol-phosphonic acids were shown to anchor gold nanoparticles selectively to hafnium-modified silicon dioxide in our previous work.[22] In those studies, the thiol-phosphonic acid functionalized nanoparticles adsorbed preferentially onto patterns of hafnium-modified SiO_2 rather than onto the surrounding bare SiO_2 surface. Others have reported the self-assembly of alkylphosphonic acid monolayers on indium tin oxide[23,24] and a range of other oxide surfaces,[25−27] as well as on hafnium-modified SiO_2.[28]

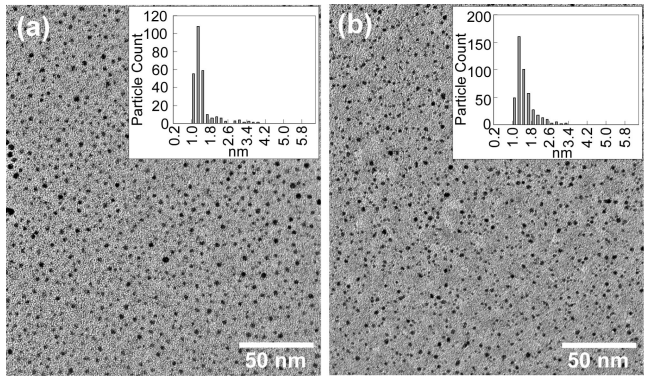

Figure 2. TEM images of gold nanoparticles (a) with PPh_3 ligand shell and (b) with 2-MEPA ligand shell. TEM images were acquired using a Philips CM12 transmission electron microscope operated at an accelerating voltage of 120 kV.

TABLE 1. TOF-SIMS Analysis of Film Composition for a Series of Immersion Times in Gold Nanoparticle Solution (Each Individual Ion Peak Intensity Has Been Normalized by the Total Ion Count)

immersion time	Zn^{2+}	Au^{3+}	PO_3^-	S^{2-}
1 s	480.6	22.8	2171.9	224.9
3 s	461.0	21.3	2115.5	200.4
10 s	455.6	21.1	2118.2	233.8
30 s	450.7	20.8	1943.9	266.3

In order to demonstrate selective self-assembly of the phosphonic acid derivatized nanoparticles, c-oriented ZnO-patterned substrates were simply immersed into a dilute aqueous solution of gold nanoparticles (0.25 mg/mL) for 10 s, and the surfaces were analyzed by time-of-flight secondary ion mass spectrometry (TOF-SIMS) imaging. Figure 3 shows TOF-SIMS images for Zn^{2+} and Au^{3+} ions on the patterned substrate, clearly verifying that the gold nanoparticles are assembled onto ZnO selectively. The ZnO surface is covered by a nanoparticle layer within 10 s, and no gold particles are observed on the bare SiO_2 substrate. Table 1 shows TOF-SIMS secondary ion yields for Zn and Au after a series of immersion times in gold nanoparticle solution. The peak intensities for ionic fragments of interest are divided by total ion intensity in each measurement to compare the relative compositions among samples. Peaks for Zn^{2+} and Au^{3+} positive ions and PO^{3-} and S^{2-} negative ions are observed even if the immersion time is only 1 s. The ratio of Au to Zn is constant and does not increase with immersion time (Table 1), suggesting the reaction time is less than 1 s. In our previous results on hafnium-modified SiO_2, the time required to achieve the maximum coverage of nanoparticles was approximately 5 days.[22] The comparatively rapid anchoring of gold nanoparticles in this case likely results from a strong electrostatic interaction between the phosphonic acid head groups and Zn atoms on the ZnO surface.

Utilizing selectively self-assembled nanoparticles as the growth catalyst offers a number of advantages over previously reported methods for nanowire growth. Because the terminal functionality of the thiol ligand shell dictates the interactions of the particles with the substrate, a number of specific and selective particle−substrate interactions can be envisioned for the generation of nanostructures derived from a wide range of seed layer materials. This and similar approaches to nanomaterials assembly will also be important in the development of green nanofabrication strat-

egies. Since this system uses only the amount of gold required to cover the seed layer, the amount of gold waste is much smaller than in vapor deposition systems. Less than 50 μL of gold nanoparticle solution (0.25 mg/mL) was used for the preparation of zinc oxide nanowires in each experiment. The mass of gold consumed is less than 12.5 μg in this case, whereas the gold source used in an evaporation system is typically around 0.2 g. Consequently, the mass of gold consumed by using dilute nanoparticle solution to selectively place the catalyst material is at least 16 000 times less than that consumed in an evaporation system for deposition of patterned gold films. In addition to using less material, the approach offers advantages for greener nanomanufacturing[29] because it eliminates the need for high vacuum deposition processes and is compatible with additive fabrication strategies.

Having shown the selective assembly of nanoparticles onto patterned ZnO seed layers, we next generated zinc oxide nanowire arrays through the VLS method using the assembled particles as the growth catalyst and structurally characterized the arrays using scanning electron microscopy (SEM). Figure 4 shows SEM images of VLS-deposited ZnO nanowires grown on the nanoparticle-modified ZnO seed layer. ZnO nanowire arrays grow vertically only on the patterned gold nanoparticle/ZnO layer and not on the surrounding base substrate. The regions of growth correlate with gold patterns observed by TOF-SIMS mapping (Figure 3a,b). Thus, the nanoparticle-modified seed layer indeed serves as a selective template for nanowire growth. The average diameter and height of ZnO nanowires are 30 (±10 nm) and 1 μm, respectively. The height of the ZnO nanowires is controllable from 100 nm to a few micrometers by varying the growth time. Figure 5 shows SEM images of ZnO grown by VLS with and without deposition of nanoparticles onto the seed layer. ZnO structures are observed on all the substrates examined, except for bare SiO_2 (Figure 5a). The VLS-deposited ZnO without gold nanoparticle modification shows the hexagonal columnar structure of ZnO (Figure 5b), while the nanoparticle-modified ZnO shows a nanowire array (Figure 5c). These results indicate that the assembled gold nanoparticle film works as a catalyst for the growth of ZnO nanowires, while seed layers void of nanoparticle films show no nanowire growth.

In addition to verifying the importance of both the seed layer and the nanoparticle catalysts for generating nanowire arrays, we were able to characterize the effect of the base substrate on the structural quality of the nanowires. Figure 5c shows the nanowire arrays on SiO_2 are tilted slightly relative to the surface normal and are not uniformly parallel. The nonuniform orientation of nanowires reflects the quality of ZnO seed layer on the nonepitaxial underlying substrate. The [0001] orientation of ZnO seed layers are confirmed by XRD.

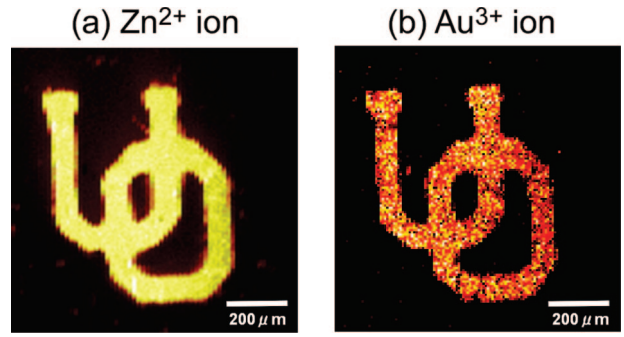

Figure 3. TOF-SIMS images for Zn^{2+} and Au^{3+} ions. TOF-SIMS images were acquired with an ION-TOF Model IV spectrometer using a bismuth liquid metal ion gun as the primary ion beam, operated in the positive polarity mode.

Figure 6 shows the X-ray θ-rocking curve of the (0002) peak for the ZnO seed layer on SiO_2 and c-sapphire substrates. This measurement is used for determining the orientation distribution of the crystals in the seed layer.[30] The intensity of the peak for the ZnO seed layer on c-sapphire (Figure 6b) is three times higher and the full width at half-maximum (fwhm) much narrower than that observed for the ZnO seed layer on SiO_2 (Figure 6a). These differences suggest that the ZnO seed layer on c-sapphire has higher crystallinity and smaller orientation distribution than that on SiO_2. Figure 5d shows a vertical nanowire array on a c-sapphire substrate with a nanoparticle-modified ZnO layer. The alignment of the nanowires is more uniformly parallel and perpendicular to the underlying epitaxial substrate, demonstrating that high-quality ZnO nanowire arrays can be generated by this approach.

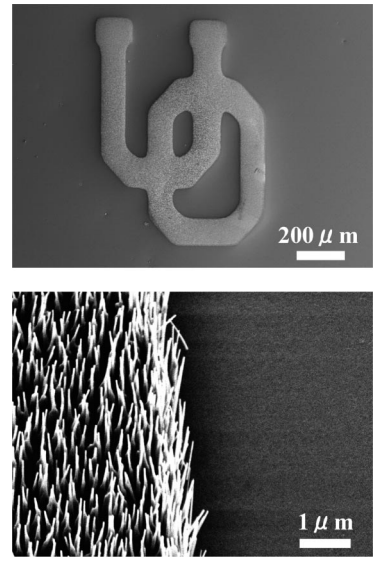

Figure 4. SEM images of VLS-deposited ZnO grown after immersion of substrates into the gold nanoparticle solution for 10 s. The images at (a) low magnification and (b) high magnification with a 30° tilt angle clearly show the growth of a zinc oxide nanowire array on the patterned seed layer. SEM images were acquired with a Zeiss Ultra scanning electron microscope operated at an accelerating voltage of 5 kV.

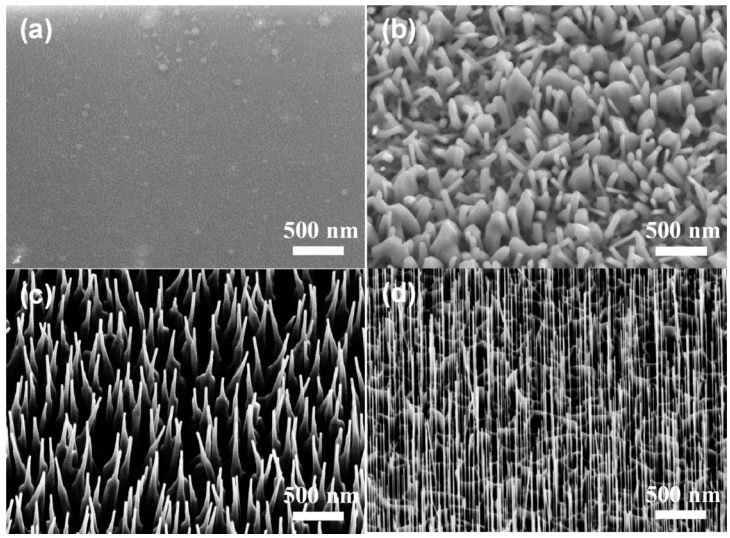

Figure 5. SEM images of VLS-grown ZnO (a) on SiO_2, (b) on an unmodified ZnO seed layer, (c) on a gold nanoparticle-modified ZnO seed layer on SiO_2, and (d) on a nanoparticle-modified ZnO seed layer on c-sapphire. SEM images were acquired with a Zeiss Ultra scanning electron microscope operated at an accelerating voltage of 5 kV.

In order to further assess the quality of the nanowire arrays generated by the VLS method utilizing selectively self-assembled gold nanoparticles as the growth catalyst, we examined their photoluminescence behavior. Photoluminescence (PL) measurements were performed at 77 K in the backscattering geometry by excitation with the 325 nm line of a He−Cd laser. Figure 7 shows PL spectra of VLS-grown ZnO on each of the aforementioned substrates. Only samples with nanowires (Figure 7c,d) show strong photoemission peaks. The narrow UV peaks located around 3.3 eV indicate exciton recombinations.[14,20] The broad green emission peak located around 2.5 eV results from the recombination of photogenerated holes with singly ionized oxygen site defects.[8] The nanowire array on c-sapphire shows stronger UV emission peaks and a smaller green emission peak than the nanowire array on SiO_2. These differences in photoemission indicate that the epitaxial ZnO nanowires on c-sapphire have fewer defects and/or dislocations than the nonepitaxial nanowires on the SiO_2 base substrate.

Figure 8 shows high-resolution PL spectra of near-band-edge emission on a semilogarithmic scale. Six peaks are observed in the spectrum. The peak at 3.371 eV is attributed to the free exciton recombination (FE).[8,31] The next peak (3.353 eV) results from bound exciton (BE) recombination.[8] The energy separation of these two peaks is 18 meV in our measurements, which is in general agreement with the reported value of 15−20 meV for the biexciton binding energy of ZnO.[8,32,33] Although all of these samples show BE emissions, only nanowire samples (Figure 8c,d) exhibit FE recombination peaks. The epitaxial nanowire array on sapphire shows a higher FE recombination peak intensity than the nonepitaxial nanowires on SiO_2, but it is difficult to compare the absolute peak intensities using Figure 8 because the data are on a semilogarithmic scale. The ratio between the FE and BE peak intensities can be used to compare the two different nanowire samples, as an array with a greater number of defects will have a more intense BE peak relative to the FE peak. The ratio of the FE peak intensity to the BE emission peak intensity is greater for the epitaxial nanowire array on c-sapphire than for the nonepitaxial array on SiO_2 ($I_{FE}/I_{BE} = 1.20$ for the epitaxial nanowires and 0.97 for the nonepitaxial nanowires, Figure 8d). In addition,

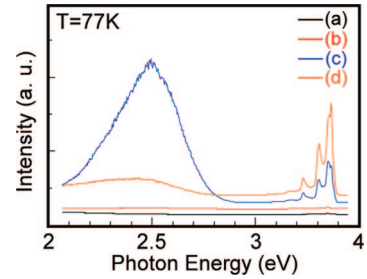

Figure 7. Photoluminescence spectra of VLS-grown ZnO (a) on SiO_2, (b) on an unmodified ZnO seed layer, (c) on a gold nanoparticle-modified ZnO seed layer on SiO_2, and (d) on a gold nanoparticle-modified ZnO seed layer on c-sapphire. Photoluminescence measurements were carried out using the 325 nm line of a He−Cd laser. The emission power was 6 mW. The angle between the incident laser and the substrate was 45°. The PL detector faced the substrates vertically.

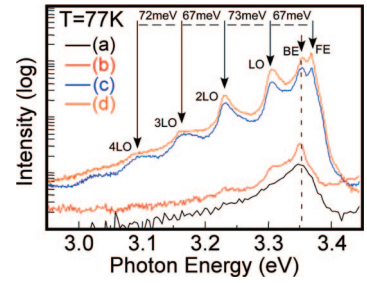

Figure 8. High-resolution photoluminescence spectra of the near-band-edge emission of VLS-grown ZnO (a) on SiO_2, (b) on an unmodified ZnO seed layer, (c) on a gold nanoparticle-modified ZnO seed layer on SiO_2, and (d) on a gold nanoparticle-modified ZnO seed layer on c-sapphire. (The intensity is on a semilogarithmic scale.)

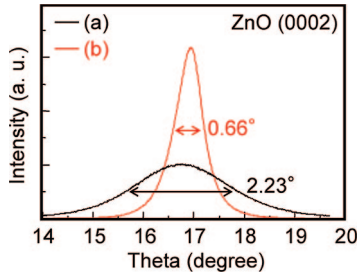

Figure 6. X-ray rocking curve of (0002) for ZnO seed layer (a) on SiO_2 and (b) c-sapphire substrates. The angle 2θ was fixed at the ZnO (0002) peak observed for these samples (34.30°).

there are four peaks at 3.304, 3.231, 3.164, and 3.092 eV with similar spacing for the nanowire samples (Figure 8c,d). The average value of the energy separations between adjacent peaks, including the FE peak, is approximately 70 meV. This value corresponds to the energy for the longitudinal optical (LO) phonon in ZnO single crystals (73 meV).[31,34] It is generally accepted as the radiative recombination of the LO phonon replicas by the free exciton−phonon coupling effect.[31,34] The PL with exciton−phonon coupling has been reported for ZnO high-quality epitaxial films[31,32,34] and for thin nanowires.[8] Taken together, the results from our PL measurements suggest that the selective self-assembly system is suitable for developing patterned optical devices using ZnO nanowires on epitaxial substrates.

In summary, the selective anchoring of gold nanoparticles enables patterned growth of ZnO nanowire arrays. A layer of phosphonic acid functionalized gold nanoparticles is assembled onto a ZnO seed layer in less than 1 s and is used as the catalyst in the VLS growth of ZnO nanowires. The obtained vertical ZnO nanowire arrays show strong UV luminescence with near-band-edge energy, and the as-grown epitaxial nanowire arrays on c-sapphire substrates show strong FE recombination emission without annealing. User-defined arrays of this sort should be useful for sensors and field emission devices, as well as light emitting devices. This self-assembled system can incorporate many different selective ligand−substrate interactions based on well-known surface chemistries. Therefore, it should be useful for fabricating a range of oxide, nitride, and carbon nanostructures that are generated utilizing metal catalysts. Finally, this growth technique offers benefits for low-cost, low-waste manufacturing, and such methods are becoming increasingly important in the development of green nanofabrication strategies. We are currently investigating whether this approach enables tuning of nanowire diameter and spacing through control of nanoparticle core diameter, ligand shell length, and growth temperature.

METHODS

Gold nanoparticles ($d_{core} \approx 1.5$ nm) were synthesized and functionalized with 2-mercaptoethylphosphonic acid (2-MEPA) as described previously.[35,36] Briefly, hydrogen tetrachloroaurate trihydrate ($HAuCl_4 \cdot 3H_2O$, 1.00 g, 2.54 mmol) in water reacts with triphenylphosphine (PPh_3, 2.33 g, 8.88 mmol) in toluene in the presence of the phase-transfer catalyst tetraoctylammonium bromide (TOAB, 1.40 g, 2.56 mmol). Reduction with $NaBH_4$ (1.99 g, 52.6 mmol) yields 1.5 nm (±0.4 nm) PPh_3-stabilized gold nanoparticles. The PPh_3-stabilized particles were dissolved in dichloromethane, mixed with one mass equivalent of 2-MEPA dissolved in water, and stirred for 48 h. When the organic layer was nearly colorless, the aqueous layer was collected and washed with dichloromethane (3 × 50 mL). Excess 2-MEPA was removed from the crude product solution by diafiltration using a 10 kD diafiltration capsule (Pall Life Sciences) and approximately 50 volume equivalents of deionized water.[37] Nanoparticles were considered pure when no free ligand was evident by ^{1}H NMR. The product was lyophilized overnight, leaving a dark brown product. The product was dissolved in deionized water to achieve the desired concentration for substrate soaking solutions.

ZnO seed films were prepared by spin casting a sol−gel precursor onto Si wafers with a 3 μm thermal SiO_2 layer, followed by an annealing step. The synthesis of a sol−gel precursor for ZnO has been reported by Kamalasanan *et al.*[38] Zinc acetate dihydrate ($(CH_3COO)_2Zn \cdot 2H_2O$) (5 g, 22 mmol) was dissolved in 2.5 mL of ethylene glycol, and the mixture was heated at 150 °C for 15 min in a round-bottom flask equipped with a reflux condensor. After cooling the transparent solution to room temperature, 8 mL of 1-propanol and 0.2 mL of glycerol were added, followed by 5 mL of triethylamine and 0.1 mL of water. The resulting solution was stirred at 35 °C for 30 h. This precursor solution was diluted with isopropanol to a concentration of 50 mM. ZnO seed layer films were prepared by spin casting this solution at 3000 rpm for 60 s onto a 1 cm^2 wafer. The spin-coated films were prebaked at 150 °C for 10 min to drive off solvent and then baked at 350 °C for 30 min to obtain c-oriented ZnO seed films. Patterned ZnO seed films were prepared by photolithographic patterning of the substrate using Shipley 1818 photoresist. The resist is spin-cast onto a silicon wafer at 3000 rpm for 60 s and heated at 100 °C for 60 s to drive off residual solvent. The substrate is then placed under a prefabricated emulsion mask using an OAI Model 200 Contact Mask Aligner and exposed to UV light for 10−12 s (125 W/cm^2). The photoresist patterns are developed by soaking the substrate in an agitated mixture of 3.5:1 deionized water: Microposit 351 Developer for 60 s. The substrates are rinsed again in deionized water and dried under a stream of nitrogen. The patterned substrates were heated at 120 °C for 1 h to improve the adhesion of the photoresist to the substrate. The photopatterning procedure is followed by ZnO seed film deposition and lift-off of the photoresist in acetone prior to annealing the ZnO films at 350 °C for 30 min. Patterned ZnO surfaces were treated with UV−ozone for 5 min and rinsed with deionized water to remove adventitious carbon contamination[39] prior to immersion in an aqueous gold nanoparticle solution (0.25 mg/mL). The samples were rinsed with copious amounts of deionized water to remove any physisorbed nanoparticles and then dried under a stream of nitrogen prior to further surface modification or analysis.

ZnO nanowire arrays were grown by the VLS method. A mixture of ZnO and carbon powder (roughly 1:1 by mass) was placed in a small quartz tube as a ZnO source, and the ZnO substrate was placed downstream from the source. The substrate temperature was held constant at 600 °C. The source temperature was raised to 900 °C and maintained at that temperature for 20 min in N_2 gas flow (2.5 SCFH). Then, the furnace was shut down and cooled to room temperature while maintaining the nitrogen flow.

Acknowledgment. We thank Dr. Stephen Golledge for assistance in acquiring all TOF-SIMS data reported in this work. We gratefully acknowledge Sony Corporation (Japan), the National Science Foundation IGERT program (DGE-0114419), and the Air Force Research Laboratory (under agreement number FA8650-05-1-5041) for their support on this research.

REFERENCES AND NOTES

1. Brust, M.; Kiely, C. J. Some Recent Advances in Nanostructure Preparation from Gold and Silver Particles: A Short Topical Review. *Colloids Surf. A* **2002**, *202*, 175–186.
2. Oldenburg, S. J.; Averitt, R. D.; Westcott, S. L.; Halas, N. J. Nanoengineering of Optical Resonances. *Chem. Phys. Lett.* **1998**, *288*, 243–247.
3. Braun, E.; Eichen, Y.; Sivan, U.; Ben-Yoseph, G. DNA-templated Assembly and Electrode Attachment of a Conducting Silver Wire. *Nature* **1998**, *391*, 775–778.

4. Gunter, P. L. J.; Niemantsverdriet, J. W.; Ribeiro, F. H.; Somorjai, G. A. Surface Science Approach to Modeling Supported Catalysts. *Catal. Rev.—Sci. Eng.* **1997**, *39*, 77–168.
5. Li, Y; Meng, G. W.; Zhang, L. D.; Phillipp, F. Ordered Semiconductor ZnO Nanowire Arrays and Their Photoluminescence Properties. *Appl. Phys. Lett.* **2000**, *76*, 2011–2013.
6. Lao, J. Y.; Wen, J. G.; Ren, Z. F. Hierarchical ZnO Nanostructures. *Nano Lett.* **2002**, *2*, 1287–1291.
7. Vayssieres, L. Growth of Arrayed Nanorods and Nanowires of ZnO from Aqueous Solutions. *Adv. Mater.* **2003**, *15*, 464–466.
8. Yao, B. D.; Chan, Y. F.; Wang, N. Formation of ZnO Nanostructures by a Simple Way of Thermal Evaporation. *Appl. Phys. Lett.* **2002**, *81*, 757–759.
9. Huang, M. H.; Mao, S.; Feick, H.; Yan, H. Q.; Wu, Y. Y.; Kind, H.; Weber, E.; Russo, R.; Yang, P. D. Room-Temperature Ultraviolet Nanowire Nanolasers. *Science* **2001**, *292*, 1897–1899.
10. Kong, Y. C.; Yu, D. P.; Zhang, B.; Fang, W.; Feng, S. Q. Ultraviolet-Emitting ZnO Nanowires Synthesized by a Physical Vapor Deposition Approach. *Appl. Phys. Lett.* **2001**, *78*, 407–409.
11. Lee, C. J.; Lee, T. J.; Lyu, S. C.; Zhang, Y.; Ruh, H.; Lee, H. J. Field Emission from Well-Aligned Zinc Oxide Nanowires Grown at Low Temperature. *Appl. Phys. Lett.* **2002**, *81*, 3648–3650.
12. Ng, H. T.; Han, J.; Yamada, T.; Nguyen, P.; Chen, Y. P.; Meyyappan, M. Single Crystal Nanowire Vertical Surround-Gate Field-Effect Transistor. *Nano Lett.* **2004**, *4*, 1247–1252.
13. Arnold, M. S.; Avouris, P.; Pan, Z. W.; Wang, Z. L. Field-Effect Transistors Based on Single Semiconducting Oxide Nanobelts. *J. Phys. Chem. B* **2003**, *107*, 659–663.
14. Johnson, J. C.; Knutsen, K. P.; Yan, H. Q.; Law, M.; Zhang, Y. F.; Yang, P. D.; Saykally, R. J. Ultrafast Carrier Dynamics in Single ZnO Nanowire and Nanoribbon Lasers. *Nano Lett.* **2004**, *4*, 197–204.
15. Bai, X. D.; Wang, E. G.; Gao, P. X.; Wang, Z. L. Measuring the Work Function at a Nanobelt Tip and at a Nanoparticle Surface. *Nano Lett.* **2003**, *3*, 1147–1150.
16. Park, J. Y.; Yun, Y. S.; Hong, Y. S.; Oh, H.; Kim, J. J.; Kim, S. S. Synthesis, Electrical and Photoresponse Properties of Vertically Well-Aligned and Epitaxial ZnO Nanorods on GaN-Buffered Sapphire Substrates. *Appl. Phys. Lett.* **2005**, *87*, 123108.
17. Zhang, Y.; Jia, H. B.; Wang, R. M.; Chen, C. P.; Luo, X. H.; Yu, D. P.; Lee, C. J. Low-Temperature Growth and Raman Scattering Study of Vertically Aligned ZnO Nanowires on Si Substrate. *Appl. Phys. Lett.* **2003**, *83*, 4631–4633.
18. Greene, L. E.; Law, M.; Tan, D. H.; Montano, M.; Goldberger, J.; Somorjai, G.; Yang, P. D. General Route to Vertical ZnO Nanowire Arrays Using Textured ZnO Seeds. *Nano Lett.* **2005**, *5*, 1231–1236.
19. Wang, X. D.; Summers, C. J.; Wang, Z. L. Large-Scale Hexagonal-Patterned Growth of Aligned ZnO Nanorods for Nano-optoelectronics and Nanosensor Arrays. *Nano Lett.* **2004**, *4*, 423–426.
20. Kim, S. W.; Fujita, S.; Fujita, S. ZnO Nanowires with High Aspect Ratios Grown by Metalorganic Chemical Vapor Deposition Using Gold Nanoparticles. *Appl. Phys. Lett.* **2005**, *86*, 153119.
21. Kunat, M.; St. Girol, G.; Burghaus, U.; Woll, Ch. The Interaction of Water with the Oxygen-Terminated, Polar Surface of ZnO. *J. Phys. Chem. B* **2003**, *107*, 14350–14356.
22. Foster, E. W.; Kearns, G. J.; Goto, S.; Hutchison, J. E. Patterned Gold-Nanoparticle Monolayers Assembled on the Oxide of Silicon. *Adv. Mater.* **2005**, *17*, 1542–1545.
23. Brewer, S. H.; Brown, D. A.; Franzen, S. Formation of Thiolate and Phosphonate Adlayers on Indium-Tin Oxide: Optical and Electronic Characterization. *Langmuir* **2002**, *18*, 6857–6865.
24. Gardner, T. J.; Frisbie, C. D.; Wrighton, M. S. Systems for Orthogonal Self-Assembly of Electroactive Monolayers on Au and ITO—An Approach to Molecular Electronics. *J. Am. Chem. Soc.* **1995**, *117*, 6927–6933.
25. Gao, W.; Dickinson, L.; Grozinger, C.; Morin, F. G.; Reven, L. Self-Assembled Monolayers of Alkylphosphonic Acids on Metal Oxides. *Langmuir* **1996**, *12*, 6429–6435.
26. Gawalt, E. S.; Avaltroni, M. J.; Koch, N.; Schwartz, J. Self-Assembly and Bonding of Alkanephosphonic Acids on the Native Oxide Surface of Titanium. *Langmuir* **2001**, *17*, 5736–5738.
27. Raman, A.; Dubey, M.; Gouzman, I.; Gawalt, E. S. Formation of Self-Assembled Monolayers of Alkylphosphonic Acid on the Native Oxide Surface of SS316L. *Langmuir* **2006**, *22*, 6469–6472.
28. Zeppenfeld, A. C.; Fiddler, S. L.; Ham, W. K.; Klopfenstein, B. J.; Page, C. J. Variation of Layer Spacing in Self-Assembled Hafnium-1,10-Decanediylbis(Phosphonate) Multilayers as Determined by Ellipsometry and Grazing Angle X-ray Diffraction. *J. Am. Chem. Soc.* **1994**, *116*, 9158–9165.
29. Hutchison, J. E. Greener Nanoscience: A Proactive Approach to Advancing Applications and Reducing Implications of Nanotechnology. *ACSNano* **2008**, *2*, 395–402.
30. Lee, D. Y.; Choi, C. H.; Kim, S. H. Growth and Characterization of ZnO Film on Si(111) Substrate by Helicon Wave Plasma-Assisted Evaporation. *J. Crystal Growth* **2004**, *268*, 184–191.
31. Ogata, K.; Kawanishi, T.; Maejima, K.; Sakurai, K.; Fujita, S.; Fujita, S. Improvements of ZnO Qualities Grown by Metal-Organic Vapor Phase Epitaxy Using a Molecular Beam Epitaxy Grown ZnO Layer as a Substrate. *Jpn. J. Appl. Phys.* **2001**, *40*, L657–L659.
32. Ko, H. J.; Chen, Y. F.; Yao, T.; Miyajima, K.; Yamamoto, A.; Goto, T. Biexciton Emission from High-Quality ZnO Films Grown on Epitaxial GaN by Plasma-Assisted Molecular-Beam Epitaxy. *Appl. Phys. Lett.* **2000**, *77*, 537–539.
33. Sun, H. D.; Makino, T.; Segawa, Y.; Kawasaki, M.; Ohtomo, A.; Tamura, K.; Koinuma, H. Biexciton Emission from $ZnO/Zn_{0.74}Mg_{0.26}O$ Multiquantum Wells. *Appl. Phys. Lett.* **2001**, *78*, 3385–3387.
34. Sans, J. A.; Segura, A.; Mollar, M.; Mari, B. *Thin Solid Films* **2004**, *453*, 251–255.
35. Weare, W. W.; Reed, S. M.; Warner, M. G.; Hutchison, J. E. Improved Synthesis of Small ($d_{core} \approx 1.5$ nm) Phosphine-Stabilized Gold Nanoparticles. *J. Am. Chem. Soc.* **2000**, *122*, 12890–12891.
36. Hutchison, J. E.; Foster, E. W.; Warner, M. G.; Reed, S. M.; Weare, W. W.; Buhro, W.; Yu, H. Triphenylphosphine-Stabilized Gold Nanoparticles. *Inorg. Synth.* **2004**, *34*, 228–232.
37. Sweeney, S. F.; Woehrle, G. H.; Hutchison, J. E. Rapid Purification and Size Separation of Gold Nanoparticles *via* Diafiltration. *J. Am. Chem. Soc.* **2006**, *128*, 3190–3197.
38. Kamalasanan, M. N.; Chandra, S. Sol−Gel Synthesis of ZnO Thin Films. *Thin Solid Films* **1996**, *288*, 112–115.
39. Ip, K.; Gila, B. P.; Onstine, A. H.; Lambers, E. S.; Heo, Y. W.; Baik, K. H.; Norton, D. P.; Pearton, S. J.; Kim, S.; LaRoche, J. R.; Ren, F. Improved Pt/Au and W/Pt/Au Schottky Contacts on n-Type ZnO Using Ozone Cleaning. *Appl. Phys. Lett.* **2004**, *84*, 5133–5135.